



Published in final edited form as:

Arch Biochem Biophys. 2011 March 1; 507(1): 111–118. doi:10.1016/j.abb.2010.11.001.

Molecular Probes of the Mechanism of Cytochrome P450.

Oxygen Traps a Substrate Radical Intermediate

Harriet L. R. Cooper and John T. Groves*

Department of Chemistry, Princeton University, Princeton NJ 08544 USA

Abstract

The diagnostic substrate tetramethylcyclopropane (TMCP) has been reexamined as a substrate with three drug- and xenobiotic-metabolizing cytochrome P450 enzymes, human CYP2E1, CYP3A4 and rat CYP2B1. The major hydroxylation product in all cases was the unrearranged primary alcohol along with smaller amounts of a rearranged tertiary alcohol. Significantly, another ring-opened product, diacetone alcohol, was also observed. With CYP2E1 this product accounted for 20% of the total turnover. Diacetone alcohol also was detected as a product from TMCP with a biomimetic model catalyst, FeTMPyP, but not with a ruthenium porphyrin catalyst. Lifetimes of the intermediate radicals were determined from the ratios of rearranged and unrearranged products to be 120, 13 and 1 ps for CYP2E1, CYP3A4 and CYP2B1, respectively, corresponding to rebound rates of $0.9 \times 10^{10} \text{ s}^{-1}$, $7.2 \times 10^{10} \text{ s}^{-1}$ and $1.0 \times 10^{12} \text{ s}^{-1}$. For the model iron porphyrin, FeTMPyP, a radical lifetime of 81 ps and a rebound rate of $1.2 \times 10^{10} \text{ s}^{-1}$ were determined. These apparent radical lifetimes are consistent with earlier reports with a variety of CYP enzymes and radical clock substrates, however, the large amounts of diacetone alcohol with CYP2E1 and the iron porphyrin suggest that for these systems a considerable amount of the intermediate carbon radical is trapped by molecular oxygen. These results add to the view that cage escape of the intermediate carbon radical in $[\text{Fe}^{\text{IV}}\text{-OH}\cdot\text{R}]$ can compete with cage collapse to form a CO bond. The results could be significant with regard to our understanding of iron-catalyzed C-H hydroxylation, the observation of P450-dependent peroxidation and the development of oxidative stress, especially for CYP2E1.

Introduction

Cytochrome P450 enzymes (CYP) comprise a large, important and highly versatile class of heme-thiolate proteins. [1] Understanding the mechanisms of action of cytochrome P450 with its substrates continues to be a central concern with regard to phase I drug metabolism and xenobiotic toxicity. [2,3] Metabolites may be toxic or they may have enhanced bioactivity. [4] Indeed, modern drug discovery requires the identification and characterization of toxic metabolites early in the development pipeline. [5,6] CYP enzymes are known to mediate a wide variety of oxidative transformations, including N-, O- and S-dealkylations, heteroatom oxygenations, desaturations, deformylations and epoxidations. However, the ability of CYPs to catalyze the oxygenation of even strong C-H bonds, which is chemically the most extraordinary, have received the greatest mechanistic [7] and theoretical [8] attention. More generally, cytochrome P450 stands as a paradigm of oxidative

jtgroves@princeton.edu.

Publisher's Disclaimer: This is a PDF file of an unedited manuscript that has been accepted for publication. As a service to our customers we are providing this early version of the manuscript. The manuscript will undergo copyediting, typesetting, and review of the resulting proof before it is published in its final citable form. Please note that during the production process errors may be discovered which could affect the content, and all legal disclaimers that apply to the journal pertain.

catalysis mediated by a first-row transition metal with many lessons to offer regarding C-H bond activation and our basic notions of chemical reaction mechanisms, electronic structure and reactivity. [7–10]

The consensus mechanism for C-H hydroxylation by cytochrome P450 is shown in Scheme 1. There is abundant evidence for the early stages of the reaction cycle, leading from the resting ferric form of the heme site through the reduced, oxygenated, peroxy and hydroperoxy states. The accumulated spectroscopic evidence has been extensively reviewed. [7,9,11]

The *oxygen rebound* mechanism for P450-mediated hydroxylations, involving C-H abstraction by a ferryl heme intermediate (compound I) first emerged from our studies with model iron systems. [12,13] In 1978, [14] we showed in collaboration with Jud Coon that a reconstituted P450 system hydroxylated the simple but informative hydrocarbon substrate norbornane at C2 with significant loss of stereochemistry at the oxygenation site. [15–17] We interpreted this outcome to be indicative of a hydrogen abstraction-radical recombination mechanism. In subsequent years, aliphatic hydroxylations by P450 enzymes were found to be accompanied by a range of molecular rearrangements supporting the idea of intermediate, but transient, carbon-centered radicals. Modes of rearrangements that were observed include allylic rearrangement, [18] cyclopropyl-carbinyl-homoallyl rearrangements, [19] C-C fragmentation, [20] and epimerizations. [21] In parallel model studies, we showed that synthetic oxoiron(IV) porphyrin radical cation complexes, [22,23] as well as oxochromium, oxomanganese and oxoruthenium analogs, [10,24] could be prepared and spectroscopically characterized by a variety of techniques. These studies showed that such species mimicked P450 reactivity in a variety of ways. Significantly, recent studies with model, water-soluble iron porphyrins have shown that a very reactive oxoiron(IV) porphyrin radical cation $[O=Fe^{IV}P^+]$ could be prepared via peroxyacid oxidation of iron(III) precursors that are able to hydroxylate C-H bonds at extraordinary rates ($>10^6 M^{-1}, s^{-1}$). [25]

The reactive P450 intermediates after the ferric-hydroperoxy state have proven to be much more elusive. Studies of P450 reactions with peroxyacids by Egawa, [26] Dawson and Ballou, [27] and Sligar [28] have supported the view that the oxidizing species of P450 is a particularly reactive, thiolate-ligated, oxoiron(IV) porphyrin radical cation $[O=Fe^{IV}P^+]$ analogous to the well-characterized compound I of chloroperoxidase, [29] although the preparation of the P450 compound I intermediate in those studies was difficult to characterize. Newcomb et al. have offered evidence that a reactive CYP119 species with a visible spectrum very much like the resting ferric protein could be generated by laser flash photolysis. [30] However, there is debate over the nature of the precursor that was photolyzed, since the method of production via peroxyacids could lead either to a compound II species, $PFe^{IV}-OH$, [31] or a ferric nitrosyl, $Fe^{III}-NO$. [32] There has also been debate regarding the method of data analysis for the UV difference spectra used in these studies. Green has presented an analysis of these methods with the conclusion that the ferric-protein-like intermediate reported by Newcomb is not compound I of P450 [33] Very recently, Rittle and Green have reported clear evidence that the actual reactive intermediate of CYP119 does, indeed, look like the oxoFe(IV) porphyrin radical cation (compound I) of chloroperoxidase. [34] A high yield of the CYP119 compound I was obtained by carefully tuning the peroxyacid oxidation of the resting ferric enzyme. The authentic CYP119 compound I had a strongly blue-shifted Soret band with diminished intensity and a broad absorption near 700 nm, as is characteristic of oxoFe(IV) porphyrin radical cations. The Mössbauer spectrum of freeze-quenched samples of the intermediate was similar to that of CPO compound I. The EPR consistent with an $S=1$ ferryl $[Fe(IV)=O]$ spin coupled to a porphyrin radical to afford a net $S=1/2$ ground state. Significantly, this CYP119 compound I

intermediate was able to hydroxylate unactivated C-H bonds with very fast apparent rate constants in the range of 10^4 – 10^7 $M^{-1}s^{-1}$. Clearly, the study of the nature of active oxygen species involved in cytochrome P450 catalysis continues to be a lively and informative field.

In the present study we have compared the reactions of several P450 isozymes with the diagnostic substrate probe, tetramethylcyclopropane (TMCP). CYP3A4 is the most abundant P450 enzyme in the human liver and is responsible for the phase I metabolism of ~50% of prescription drugs. [35] The P450 enzymes CYP2C9, 2C19, 2D6 and CYP3A4 together account for 95% of drug metabolism. [36] Human CYP2E1, found largely in hepatocytes and epithelial cells, is known to oxidize a wide variety of low molecular weight xenobiotics as well as signaling fatty acids such as arachidonic acid. CYP2E1 metabolism is largely responsible of the cytotoxicity of acetaminophen and is implicated in oxidative stress and liver damage resulting from alcohol exposure. [37,38] Similarly, CYP2B1 is a drug metabolizing, phenobarbital-induced isozyme of rat liver microsomes.

Tetramethylcyclopropane was first used as a P450 substrate by Ingold, et al. in their pioneering development of radical clock substrates. [39,40] The ring-opening rate constant for the cyclopropylcarbinyl radical from TMCP was found to be moderately fast, 2×10^9 s^{-1} . Rat liver microsomes and a reconstituted CYP2B4 system both gave about 1% ring-opened, homoallylic alcohol, in that study, corresponding to an inferred radical lifetime of 4 ps in the oxygen rebound process.

The rationale for our reexamination of TMCP as a diagnostic P450 substrate was to see if this small substrate could afford evidence of the radical cage phenomena we had seen in the non-heme diiron hydroxylase AlkB. [41] In that case a slower radical clock produced more rearranged product than the faster clock. Such a result can be accommodated if cage-escape of an incipient radical is competitive with rebound to afford hydroxylated product. The results show that the apparent radical lifetime varies over two orders of magnitude depending upon the particular P450 isozyme used. Significantly, a new product, diacetone alcohol, was also detected. We compare these results for the three CYP enzymes with a benchmark model iron porphyrin/iodosylbenzene system, which afforded the same products.

Results

Hydroxylation of Tetramethylcyclopropane with CYP Enzymes

1,1,2,2-Tetramethylcyclopropane **1** (TMCP) was reacted with human CYP3A4 and CYP2E1, and rat CYP2B1 in a reconstituted system that also contained P450 reductase and cytochrome b5. [42] Nicotinamide adenine dinucleotide phosphate (NADPH) was used as the electron donor. TMCP turned out to be a very good substrate for the CYP enzymes employed here, with activities ranging from 90 to 2000 nmol/min/nmol P450, ~5 fold more active than is typical for standard substrates. The structures of TMCP and the observed products are depicted in Figure 1. Products **2** and **3** were identified by comparison to synthesized authentic standards. Products **4** and **5** were identified by comparison to commercially available materials. Yields were determined by comparing response factors of reaction mixtures to these standards vs. dodecane as an internal standard.

Table 1 shows the results of oxidation of tetramethylcyclopropane by the three CYP proteins. The GC-MS TIC traces of the individual reactions are shown in Figures 2 and 3. In the oxidation of TMCP by CYP2E1, the unrearranged alcohol **2** was the major product (80%). The only other product detected was a very significant amount of diacetone alcohol **5** (20%). This product was completely absent in control runs lacking NADPH (blue line). For the oxidation of TMCP by rat CYP2B1, again the unrearranged alcohol **2** was the major product (99.7%), along with 0.1% unrearranged aldehyde **3**. The rearranged alcohol **4** (0.2%

relative yield) and diacetone alcohol **5** (trace) were also detected. As such, this run served as a negative control for the production of **5** since it had all of the ingredients as the CYP2E1 run except a different P450 protein. For the oxidation of TMCP by CYP3A4 (Figure 3), the major product was the unrearranged alcohol **2** (91%), accompanied by 1.5% unrearranged aldehyde **3**. The rearranged alcohol **4** was present in 1.0% relative yield, and 1.5% diacetone alcohol **5** was also detected.

In control experiments (full reaction mixture without NADPH), products **4** and **5** were stable under the reaction conditions and were not converted to any products. TMCP was filtered through basic alumina before use to ensure removal of oxygenated impurities. Control reactions (either without enzyme, without NADPH or without both) were free of any products including **5**, which could be an autoxidation product of TMCP. Each reaction was run in the presence of both catalase (1000 units) and MnSOD (1000 units). Under these conditions the amount of diacetone alcohol product (**5**) was reduced to 7.5% for the CYP2E1 reaction. There was no effect on the CYP3A4 or CYP 2B1 reactions.

Iron porphyrin-catalyzed oxidation of 1,1,2,2-tetramethylcyclopropane (TMCP)

The oxidation of TMCP (**1**) by a model iron metalloporphyrin was also investigated. The reaction was carried out using iron(III) tetrakis-5,10,15,20-(N-methyl-4-pyridyl)-porphyrin (Fe^{III}-4-TMPyP) catalyst and iodosylbenzene as the oxidant in acetonitrile. [25] As a control of the analytical method, carbonylruthenium(II) tetrakis-5,10,15,20-pentafluorophenylporphyrin (CO)Ru^{II}(TPFPP) was used with 2,6-dichloropyridine N-oxide as the oxidant in methylene chloride solvent as we have previously described. [43] With the Fe^{III}-4-TMPyP catalyst the oxidation of TMCP gave 75% of the unrearranged primary alcohol **2**, 2% of the rearranged tertiary alcohol **4** and 12% of the autoxidation product **5** in a 1% overall conversion with excess substrate. A rearranged epoxide **6** (11%) was also detected (Figure 4). By contrast no diacetone alcohol (**5**) was detected with Ru(CO)TPFPP as the catalyst. These results afford an apparent radical lifetime of 81 ps and a radical rebound rate of $1.2 \times 10^{10} \text{ s}^{-1}$ (160 ps if **6** is counted as a rearrangement product).

Discussion

Tetramethylcyclopropane **1** (TMCP) was a good substrate for the three P450 isozymes investigated and the model iron porphyrin FeTMPyP in this study, affording reaction mixtures with two unrearranged products, the alcohol **2** and the corresponding aldehyde **3**; and products derived from cyclopropylcarbonyl-homoallyl rearrangement, the homoallylic alcohol **4** and diacetone alcohol (**5**). From the ratios of $(\mathbf{4} + \mathbf{5})/(\mathbf{2} + \mathbf{3})$ apparent radical lifetimes of 1–120 ps were calculated (Table 1), corresponding to radical rebound rates varying from $1.0 \times 10^{12} - 0.9 \times 10^{10} \text{ s}^{-1}$. These values closely match the reported range for other aliphatic cyclopropanes for P450-catalyzed hydroxylation reactions: bicyclopentane (~50 ps), [19] methylcyclopropanes (4–100 ps), [39,40] norcarane (16–50 ps), [44] thujone (8–142 ps)[21] and bicyclohexane (74–252 ps)[45]. Our observed radical lifetime (1 ps) for rat CYP2B1 was somewhat shorter than that reported by Ingold et al. [39,40] (4.0 ps) for rat liver microsomes, which are known to contain mostly CYP2B1 and CYP2B2. By contrast, the apparent radical lifetimes reported for phenylmethylcyclopropanes are notably shorter. [46,47]

Diacetone alcohol (**5**) as an oxygen-trapped product

The appearance of diacetone alcohol (**5**) among the products can be rationalized by trapping of the rearranged homoallyl radical by molecular oxygen (Scheme 2). In the metalloporphyrin-catalyzed oxidation of TMCP, product **5** was not formed in the absence of oxygen or in the presence of oxygen-radical scavengers. Control reactions without enzyme,

without NADPH or without both showed no or almost no production of **5**, ruling out significant contribution of autoxidation processes to its formation. Although, diminished yields of **5** with CYP2E1 in the presence of catalase and MnSOD suggest that some of this product may result from uncoupling of the oxygen reduction process from substrate oxygenation (Scheme 1). However, TMCP is a rather stable substrate and not prone to extensive spontaneous autoxidation due to the strong methyl C-H bonds (97 kcal/mol). [48] Indeed, the reaction of CYP2B1 with TMCP in the presence of NADPH showed almost no **5**. Accordingly, the production of **5** is most probably due to the action of the enzyme and not by non-enzymatic reactions or side reactions.

The Role of CYP2E1 in the production of radicals

CYP2E1 is involved in the metabolism of low molecular weight compounds such as ethanol, acetone, benzene and chlorobenzene. [49] CYP2E1 is induced by ethanol, and is thought to be a major contributor to liver disease among alcoholics via ethanol-induced lipid peroxidation. [38,50] The observation of **5**, the oxygen-trapped product from the TMCP radical, among the CYP2E1 metabolites suggests that radicals are formed in the catalytic cycle of this P450 enzyme. There is evidence that CYP2E1 is 'leaky', allowing radicals to escape from the active site before the completion of the oxygenation reaction. Radicals from a variety of substrates, including ethanol, [51–53] propanol and butanol, [54] carbon tetrachloride, [55] and ciprofloxacin, [56] have been trapped with spin traps such as 4-POBN [α -(4-pyridyl-1-oxide)-*N*-*tert*-butylnitrone], as shown by EPR. It has been inferred that the ethanol-derived radicals may derive from the iron dioxygen complex of CYP2E1 ($\text{Fe}^{\text{III}}\text{-O-O}\cdot$). [38] However, it has also been suggested that reactive oxygen species such as superoxide and hydrogen peroxide, rather than substrate radicals are escaping from the active site, as evidenced by the fact that the addition of the antioxidant trolox can suppress radical formation. [56] The present study does not allow a definitive assignment of the origin of the diacetone alcohol product **5**. However, carbon-carbon bond scission at the β -position of alkoxy and peroxy radicals is a common process in olefin autoxidation, [57,58] which in this case would lead to **5** and formaldehyde. The presence of MnSOD and catalase did not prevent the formation of **5** under conditions for which concentrations of both superoxide and hydrogen peroxide should have been greatly depressed. That observation, the fact that TMCP has strong C-H bonds and the detection of **5** among the products with FeTMPyP/iodosylbenzene argue that some of the substrate radicals derive from turnover at the active site and may involve the reactive ferryl species.

The crystal structure of CYP2E1 has been determined recently, both with a small, coordinating molecule at the active site and a longer fatty acid. [59,60] The substrate binding site is delineated by the heme and five nearby phenylalanines (106, 116, 207, 298, and 478) defining a volume of 190 \AA^3 . A second, smaller cavity is immediately adjacent, separated only by Phe²⁹⁸ and Phe¹⁰⁶ and a simple rotation of the phenyl appendage of Phe²⁹⁸ with no change in the I-helix, which was observed upon binding of fatty acids, more than double the size of the active site. [60] TMCP, with a molecular volume of 160 \AA^3 fits within the active site cavity but not with much room to spare (Figure 5). However, rotation of Phe²⁹⁸ could explain the apparent facility with which reduced oxygen species and substrate radicals escape from the active site of CYP2E1.

Suppression of intramolecular deuterium isotope effects for 4,4'-dimethylbiphenyl as compared to xylenes with CYP2E1 have shown that there is not enough space in the active site for the longer molecule to turn, and therefore for the two ends were not full competition with each other. [61–63] Thus, upon ring-opening of the substrate probe, the resulting homo-allyl radical may encounter restrictions in turning to complete the oxygen rebound process. Auclair et al. have reported that for norcarane, CYP2E1 showed more

rearrangement than did rat CYP2B1, bacterial P450_{CAM} or P450_{BM3}, [44] consistent with the results reported here.

Oxygen rebound as a cage recombination process

In light of the results presented here indicating that some TMCP-derived radicals live long enough to be captured by diffusion of molecular oxygen, especially for CYP2E1, it is pertinent to discuss the P450 C-H hydroxylation process in terms of a hydrogen abstraction-radical cage recombination process, as depicted in Scheme 1. To frame this discussion, the time scale of molecular vibrations is in the range of 10–100 fs and the frequency of passage of a molecular reaction such as hydrogen abstraction through a transition state is less than 200 fs. [64] A well-studied example of cage recombination and cage escape is the rebinding of NO to the heme iron of myoglobin after photodissociation. [65,66] The biphasic kinetics have been interpreted to result from very rapid NO recombination from the distal pocket within 10 ps and a slower (200 ps) binding process of NO molecules that have diffused into neighboring protein cavities. Thus, cage escape of NO competes with NO rebinding even though there is a negligible barrier to the rebinding process. Statistical mechanics simulations have shown that 5% of the NO molecules were still found in the distal pocket and in these cavities even after 1 ns. The kinetic barrier to this slower recombination phase has been associated with entropic considerations, solvent effects and the dynamics of conformational gating for diffusive return to the distal pocket.

A similar scenario can be envisioned for C-H hydroxylation by iron-containing oxygenases. The diiron alkane hydroxylase (AlkB) is a non-heme iron enzyme that is thought to have a sterically restricted active site, since it is designed to hydroxylate the terminal methyl group of n-alkanes. [67] AlkB shows a large amount of rearranged products with typical mechanistic probes such as norcarane and bicyclohexane, indicating a long-lived (~10 ns) radical intermediate. [41] A revealing aspect of that study was the observation that bicyclohexane, which is a relatively slow radical clock, afforded more radical rearranged product than norcarane. While this result is inconsistent with the typical manner that radical clock data is interpreted, the outcome is fully consistent with a competition between oxygen rebound and cage escape, or recoil, [68,69] of the incipient radical, since the recoil/rebound rate ratio will determine the extent of radical rearrangement. Such a process has the effect of masking the radical ring-opening rate. A similar phenomenon is observed in the cage escape of •NO₂ from [Fe^{IV}=O •NO₂] at the active site of myoglobin during its reaction with peroxyxynitrite. [70,71]

Applied to the cytochrome P450 enzymes in this study, CYP2B1 has shown a very short radical lifetime (1–4 ps) but with rearranged products that were still detectable. Longer apparent radical lifetimes of 13 ps for CYP3A4 and 120 ps for Cyp2E1, as well as 81 ps for the model iron porphyrin, FeTMyP, are all in the same time zone for recombination as those observed for NO recombination to myoglobin. But it is important to recognize that these radical lifetimes are all averages, with some radicals that have escaped the cage living very much longer, which could allow for trapping by freely diffusing molecular oxygen.

A more detailed description of the oxygen rebound/cage escape scenario is shown in Scheme 3. The sequence begins with the formation of the oxoiron(IV) porphyrin radical cation (compound I) intermediate (Scheme 1) with the substrate in place. The nearby water molecule is the one that is mechanistically derived from O-O bond heterolysis of the hydroperoxoiron(III) precursor (compound 0). The hydrogen abstraction is initiated by approach of the scissile C-H bond to the singly-occupied Fe-O π* orbital leading to the HAT transition state. Interestingly, the depicted water molecule has been suggested to play a role in lowering the barrier to the hydrogen atom transfer process through hydrogen bonding. [8]

Completion of the hydrogen atom transfer from carbon to the ferryl oxygen will produce a hydroxoiron(IV) intermediate (compound II). [72] The strength of the newly formed Fe^{IV}O-H bond of P450 compound II can be estimated to be ~100 kcal/mol based on the rates of hydrogen atom abstraction of a model oxoiron(IV) porphyrin cation radical. [25] Such a mechanism would suggest that the incipient substrate carbon radical would be hydrogen bonded to the oxygen of compound II. Indeed, experimental [73] and computational evidence for hydrogen bonds to alkyl radicals, especially acidic H-bond donors, [74] has been reported. The major interaction has been attributed to charge transfer from the carbon radical into the H-bond donor O-H σ^* orbital. Thus, one expects the substrate carbon radical to be stabilized by the hydrogen bond to the hydroxyl of compound II as in [R---HO-Fe^{IV}P]. Completion of the oxygen rebound process would appear to require a disruption of this hydrogen bond, such as by cage escape of the radical. As is typical of such stochastic processes, some radicals would escape the cage and rearrange while others would not. Further, the small confines of the active site, as is seen in CYP2E1, may make reencounter of the escaped radical with compound II unfavorable with respect to trapping by molecular oxygen. A hydrogen bond to the intermediate substrate radical could also explain the very short apparent radical lifetimes observed for phenylmethylcyclopropane and similar substrates, since a strong hydrogen bond could drastically change the ring-opening rate.

Summary and conclusions

We have examined the behavior of tetramethylcyclopropane as a diagnostic substrate with three important drug-metabolizing cytochrome P450 isozymes – human CYP2E1, human CYP3A4 and rat CYP2B1. The ring-opening rate of TMCP ($2 \times 10^9 \text{ M}^{-1} \text{ s}^{-1}$) has revealed radical lifetimes over the range of 1–120 ps. Significantly, the model iron porphyrin FeTMPyP/iodosylbenzene system showed amounts of substrate rearrangement commensurate with an 81 ps radical lifetime with this same substrate. The similarity of the observed behavior of the model system and the active enzymes indicate that similar mechanisms and similar intermediates are involved in both cases. These values compare well with radical lifetimes on the order of 1–250 ps observed with a variety of enzymes and radical clock substrates (Figure 6). The large variation in apparent radical lifetime observed for TMCP with these CYP enzymes shows that subtle differences in the active sites can significantly change the outcome. Both CYP2E1 and the model iron porphyrin catalyst produced a significant amount of an oxygen trapped product, diacetone alcohol (**5**). Cage escape of the radical intermediate competing with radical recombination is suggested to explain these results.

Experimental

General

Tetramethylcyclopropane and authentic standards for their oxidation products **2–6** were purchased or synthesized by literature methods.

Cytochrome P450 assays

Cytochrome P450 enzymes were purchased in insect cell microsomes from BD Biosciences (Woburn, MA). The microsomes also contained cytochrome P450 reductase (activity 2200 nmol/(min mg protein) and cytochrome b₅ (610 pmol/mg protein). For each reaction, 100 μL of Supersomes containing 100 pmol P450, 540 pmol cytochrome b₅, cytochrome P450 reductase of 200 nmol/min activity as received was added to a mixture of buffer (0.5 mL, 100 mM potassium phosphate, pH 7.4), NADPH (8 mg, 10 μmol), and substrate (1 μL , 7 μmol). This mixture was incubated in a water bath at 37 °C for 30 min. The reaction was stopped by the addition of dichloromethane (250 μL) and centrifuged for three minutes at

13750 rpm. The organic layer was separated and dried with MgSO₄, then subjected to GC-MS analysis.

Oxidation of TMCP by Synthetic Metalloporphyrins

The substrate **5** (10 μ L) in acetonitrile (200 μ L) was added to a stock solution of the porphyrin (65 μ L of 5.6 mM in acetonitrile [3.93 mg/mL Fe-4-TMPyP]), which was purchased from Mid-Century Chemical. Solid iodosylbenzene (5 mg) was added in five portions over 15 min with efficient stirring, then stirred for an additional 15 min. The reaction mixture was filtered through a short plug of silica and activated charcoal, which was rinsed with dichloromethane (200 μ L). The solution was diluted for GC-MS (around 1:100). The ruthenium porphyrin catalyst, Ru(TPFPP)(CO), was prepared and the oxidation carried out as previously described. [43]

GC-MS analysis

GC-MS analyses were run using an Agilent 7890A GC coupled to a 5975C Inert MSD with a Rtx-5Sil MS (30 m length, 0.25 mm ID, 0.25 μ m film) column. Two GC-MS thermal gradient methods were used: Method 1 started at 30 $^{\circ}$ C, holding for 6 min, ramping to 230 $^{\circ}$ C at 10 $^{\circ}$ C/min and Method 2 started at 50 $^{\circ}$ C, holding for 2 min, ramping to 230 $^{\circ}$ C at 10 $^{\circ}$ C/min. Dodecane (13 ng/mL) was added as an internal standard.

Research Highlights

Tetramethylcyclopropane reveals a range of radical lifetimes for three CYP enzymes.

A model iron porphyrin/Ar-IO system gave similar results.

Diacetone alcohol is a significant product for CYP2E1 and the model system.

Acknowledgments

We are grateful for support of this research by the National Institutes of Health (2R37 GM036298).

References

1. Ortiz de Montellano, PR. *Cytochrome P450: Structure, Mechanism and Biochemistry*. Academic/Plenum Publishers; New York: 2004.
2. Veith H, Southall N, Huang RL, James T, Fayne D, Artemenko N, Shen M, Inglese J, Austin CP, Lloyd DG, Auld DS. *Nature Biotechnology* 2009;27:1050–U1123.
3. Guengerich FP. *Chemistry & Biology* 2009;16:1215–1216. [PubMed: 20064429]
4. Lamb DC, Waterman MR, Kelly SL, Guengerich FP. *Current Opinion in Biotechnology* 2007;18:504–512. [PubMed: 18006294]
5. Obach RS. *Chemical Research in Toxicology* 2010;23:42.
6. Frederick CB, Obach RS. *Clinical Pharmacology & Therapeutics* 2010;87:345–350. [PubMed: 20107437]
7. Ortiz de Montellano PR. *Chemical Reviews* 2010;110:932–948. [PubMed: 19769330]
8. Shaik S, Cohen S, Wang Y, Chen H, Kumar D, Thiel W. *Chemical Reviews* 2010;110:949–1017. [PubMed: 19813749]
9. Ortiz de Montellano, PR.; De Voss, JJ. *Cytochrome P450 Structure, Mechanism and Biochemistry*. Ortiz de Montellano, PR., editor. Kluwer Academic/Plenum; New York: 2005. p. 183-245.
10. Groves, JT. *Cytochrome P450: Structure, Mechanism, and Biochemistry*. Ortiz de Montellano, PR., editor. Kluwer Academic/Plenum; New York: 2005. p. 1-44.

11. Denisov IG, Makris TM, Sligar SG, Schlichting I. *Chemical Reviews* 2005;105:2253–2277. [PubMed: 15941214]
12. Groves JT, McClusky GA. *Journal of the American Chemical Society* 1976;98:859–861.
13. Groves JT, Van Der Puy M. *J Am Chem Soc* 1976;98:5290.
14. Groves JT, McClusky GA, White RE, Coon MJ. *Biochemical and Biophysical Research Communications* 1978;81:154–160. [PubMed: 656092]
15. Groves, JT.; Krishnan, S.; Avaria, GE.; Nemo, TE.; Dolphin, D., et al. *Advances in Chemistry Series, No. 191. Biomimetic Chemistry. Symposium at the 177th American Chemical Society National Meeting; Honolulu, Hawaii, USA. April 2–5, 1979; Washington, D.C., USA. Illus: American Chemical Society; 1980. p. Ix+437p. 277-290.*
16. Groves JT. *Proceedings of the National Academy of Sciences of the United States of America* 2003;100:3569–3574. [PubMed: 12655056]
17. Groves JT. *Journal of Inorganic Biochemistry* 2006;100:434–447. [PubMed: 16516297]
18. Groves JT, Adhyam DV. *J Am Chem Soc* 1984;106:2177–2181.
19. Ortiz de Montellano PR, Stearns RA. *Journal of the American Chemical Society* 1987;109:3415–3420.
20. Stanjek V, Miksch M, Lueer P, Matern U, Boland W. *Angewandte Chemie-International Edition* 1999;38:400–402.
21. Jiang YY, He X, Ortiz de Montellano PR. *Biochemistry* 2006;45:533–542. [PubMed: 16401082]
22. Groves JT, Nemo TE, Myers RS. *J Am Chem Soc* 1979;101:1032–1033.
23. Groves JT, Haushalter RC, Nakamura M, Nemo TE, Evans BJ. *J Am Chem Soc* 1981;102:2884–2886.
24. Groves JT, Kruper WJ, Haushalter RC. *J Am Chem Soc* 1980;102:6377–6380.
25. Bell SR, Groves JT. *Journal of the American Chemical Society* 2009;131:9640–9641. [PubMed: 19552441]
26. Egawa T, Shimada H, Ishimura Y. *Biochemical and Biophysical Research Communications* 1994;201:1464–1469. [PubMed: 8024592]
27. Spolitat T, Dawson JH, Ballou DP. *Journal of Biological Chemistry* 2005;280:20300–20309. [PubMed: 15781454]
28. Kellner DG, Hung SC, Weiss KE, Sligar SG. *Journal of Biological Chemistry* 2002;277:9641–9644. [PubMed: 11799104]
29. Stone KL, Behan RK, Green MT. *P Natl Acad Sci USA* 2005;102:16563–16565.
30. Wang Q, Sheng X, Horner JH, Newcomb M. *J Am Chem Soc* 2009;131:10629–10636. [PubMed: 19572732]
31. Newcomb M, Halgrimson JA, Horner JH, Wasinger EC, Chen LX, Sligar SG. *Proceedings of the National Academy of Sciences of the United States of America* 2008;105:8179–8184. [PubMed: 18174331]
32. Behan RK, Hoffart LM, Stone KL, Krebs C, Green MT. *Journal of the American Chemical Society* 2007;129:5855–5859. [PubMed: 17432853]
33. Rittle J, Younker JM, Green MT. *Inorganic Chemistry* 2010;49:3610–3617. [PubMed: 20380463]
34. Rittle J, Green MT. *Science* 2010;330:xxxx.
35. Shimada T, Yamazaki H, Mimura M, Inui Y, Guengerich F. *J Pharmacol Exp Ther* 1994;270:414–423. [PubMed: 8035341]
36. Williams JA, Hyland R, Jones BC, Smith DA, Hurst S, Goosen TC, Peterkin V, Koup JR, Ball SE. *Drug Metabolism and Disposition* 2004;32:1201–1208. [PubMed: 15304429]
37. Trafalis DT, Panteli ES, Grivas A, Tsigris C, Karamanakis PN. *Expert Opinion on Drug Metabolism & Toxicology* 2010;6:307–319. [PubMed: 20073996]
38. Comporti M, Signorini C, Leoncini S, Gardi C, Ciccoli L, Giardini A, Vecchio D, Arezzini B. *Genes and Nutrition* 2010;5:101–109. [PubMed: 20606811]
39. Atkinson JK, Ingold KU. *Biochemistry* 1993;32:9209–9214. [PubMed: 8369287]
40. Bowry VW, Ingold KU. *Journal of the American Chemical Society* 1991;113:5699–5707.

41. Austin, RN.; Luddy, K.; Erickson, K.; Pender-Cudlip, M.; Bertrand, E.; Deng, D.; Buzdygon, RS.; van Beilen, JB.; Groves, JT. *Angewandte Chemie-International Edition*. Vol. 47. 2008. p. 5232-5234.
42. Pompon D. *Biochemistry* 2002;26:6429–6435. [PubMed: 3501314]
43. Wang CQ, Shalyaev KV, Bonchio M, Carofiglio T, Groves JT. *Inorganic Chemistry* 2006;45:4769–4782. [PubMed: 16749842]
44. Auclair K, Hu ZB, Little DM, Ortiz de Montellano PR, Groves JT. *Journal of the American Chemical Society* 2002;124:6020–6027. [PubMed: 12022835]
45. Austin RN, Deng DY, Jiang YY, Luddy K, van Beilen JB, Ortiz de Montellano PR, Groves JT. *Angewandte Chemie-International Edition* 2006;45:8192–8194.
46. Newcomb M, Hollenberg PF, Coon MJ. *Archives of Biochemistry and Biophysics* 2003;409:72–79. [PubMed: 12464246]
47. Newcomb M, Toy PH. *Accounts of Chemical Research* 2000;33:449–455. [PubMed: 10913233]
48. Bach RD, Dmitrenko O. *Journal of the American Chemical Society* 2004;126:4444–4452. [PubMed: 15053635]
49. Guengerich FP, Kim DH, Iwasaki M. *Chemical Research in Toxicology* 1991;4:168–179. [PubMed: 1664256]
50. Cheng ZY, Li YZ. *Chemical Reviews (Washington DC, United States)* 2007;107:748–766.
51. Reinke LA, Lai EK, Dubose CM, McCay PB. *Proceedings of the National Academy of Sciences of the United States of America* 1987;84:9223–9227. [PubMed: 2827172]
52. Albano E, Tomasi A, Goria-Gatti L, Dianzani MU. *Chemico-Biological Interactions* 1988;65:223–234. [PubMed: 2837334]
53. Minakata K, Okuno E, Nakamura M, Iwahashi H. *J Biochem* 2007;142:73–78. [PubMed: 17646184]
54. Albano E, Tomasi A, Persson JO, Terelius Y, Goriagatti L, Ingelmansundberg M, Dianzani MU. *Biochemical Pharmacology* 1991;41:1895–1902. [PubMed: 2039543]
55. Stoyanovsky DA, Cederbaum AI. *Chemical Research in Toxicology* 1999;12:730–736. [PubMed: 10458707]
56. Gurbay A, Gonthier B, Daveloose D, Favier A, Hincal F. *Free Radical Biology and Medicine* 2001;30:1118–1121. [PubMed: 11369501]
57. Boto A, Betancor C, Suarez E. *Tetrahedron Letters* 1994;35:5509–5512.
58. Birnbaum ER, Labinger JA, Bercaw JE, Gray HB. *Inorganica Chimica Acta* 1998;270:433–439.
59. Porubsky PR, Meneely KM, Scott EE. *Journal of Biological Chemistry* 2008;283:33698–33707. [PubMed: 18818195]
60. Porubsky PR, Battaile KP, Scott EE. *Journal of Biological Chemistry* 2010;285:22282–22290. [PubMed: 20463018]
61. Iyer KR, Jones JP, Darbyshire JF, Trager WF. *Biochemistry* 1997;36:7136–7143. [PubMed: 9188713]
62. Audergon C, Iyer KR, Jones JP, Darbyshire JF, Trager WF. *Journal of the American Chemical Society* 1999;121:41–47.
63. Harrelson JP, Henne KR, Alonso DOV, Nelson SD. *Biochemical and Biophysical Research Communications* 2007;352:843–849. [PubMed: 17156750]
64. Zewail AH. *Journal of Physical Chemistry A* 2000;104:5660–5694.
65. Ionascu D, Gruia F, Ye X, Yu A, Rosca F, Beck C, Demidov A, Olson JS, Champion PM. *Journal of the American Chemical Society* 2005;127:16921–16934. [PubMed: 16316238]
66. Goldbeck RA, Bhaskaran S, Ortega C, Mendoza JL, Olson JS, Soman J, Kliger DS, Esquerra RM. *Proceedings of the National Academy of Sciences, USA* 2006;103:1254–1259.
67. van Beilen JB, Smits THH, Roos FF, Brunner T, Balada SB, Röthlisberger M, Witholt B. *Journal of Bacteriology* 2005;187:85–91. [PubMed: 15601691]
68. Guallar V, Baik MH, Lippard SJ, Friesner RA. *Proceedings of the National Academy of Sciences of the United States of America* 2003;100:6998–7002. [PubMed: 12771375]

69. Guallar V, Gherman BF, Miller WH, Lippard SJ, Friesner RA. *Journal of the American Chemical Society* 2002;124:3377–3384. [PubMed: 11916423]
70. Su J, Groves JT. *Inorganic Chemistry* 2010;49:6317–6329. [PubMed: 20666389]
71. Su J, Groves JT. *J Am Chem Soc* 2009;131:12979–12988. [PubMed: 19705829]
72. Behan RK, Hoffart LM, Stone KL, Krebs C, Green MT. *Journal of the American Chemical Society* 2006;128:11471–11474. [PubMed: 16939270]
73. Merritt JM, Rudić S, Miller RE. *J Chem Phys* 2006;124:000.
74. Hammerum S. *Journal of the American Chemical Society* 2009;131:8627–8635. [PubMed: 19489573]

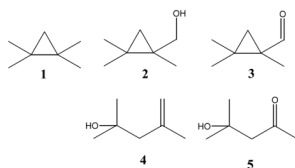


Figure 1.
Oxidation products from tetramethylcyclopropane (TMCP, **1**).

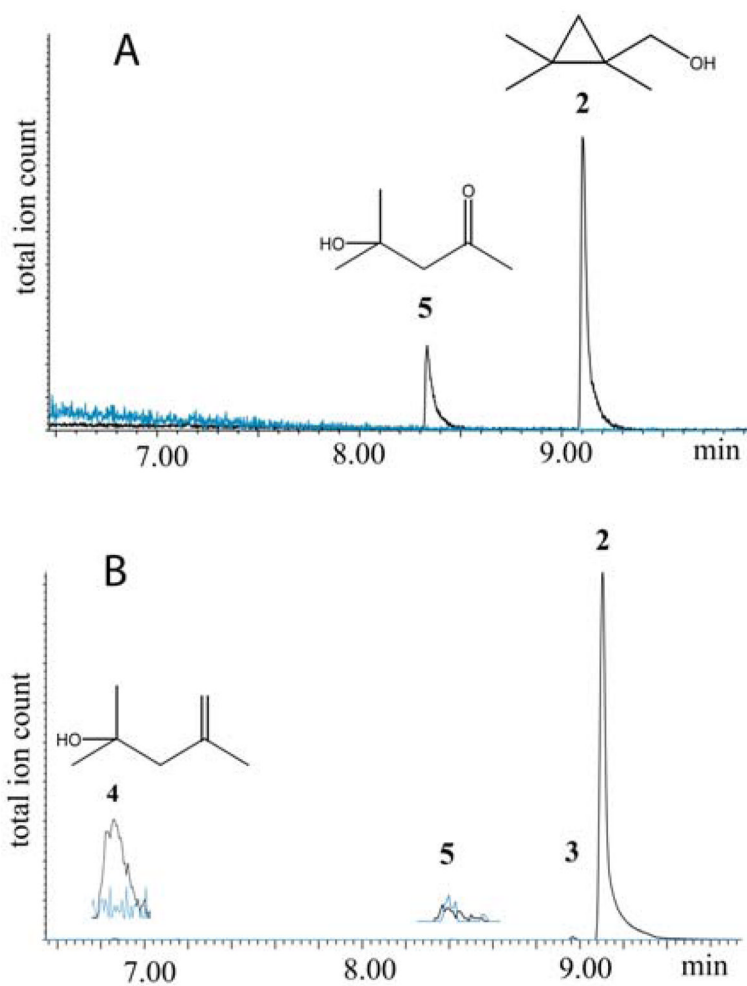


Figure 2. GC-MS total ion traces for the TMCP oxidation product region for (A) CYP2E1, (B) CYP2B1. In each trace the product run is in black and the control run, without NADPH, is in blue.

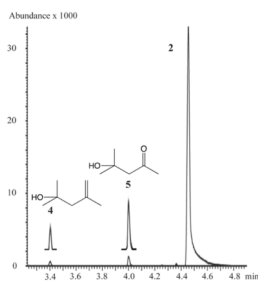


Figure 3. GC-MS total ion trace for the TMCP oxidation product region for CYP3A4 (insets are 5x).

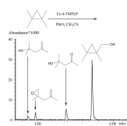


Figure 4.
Oxidation of TMCP oxidized by PhIO catalyzed by Fe-4-TMPyP in acetonitrile.

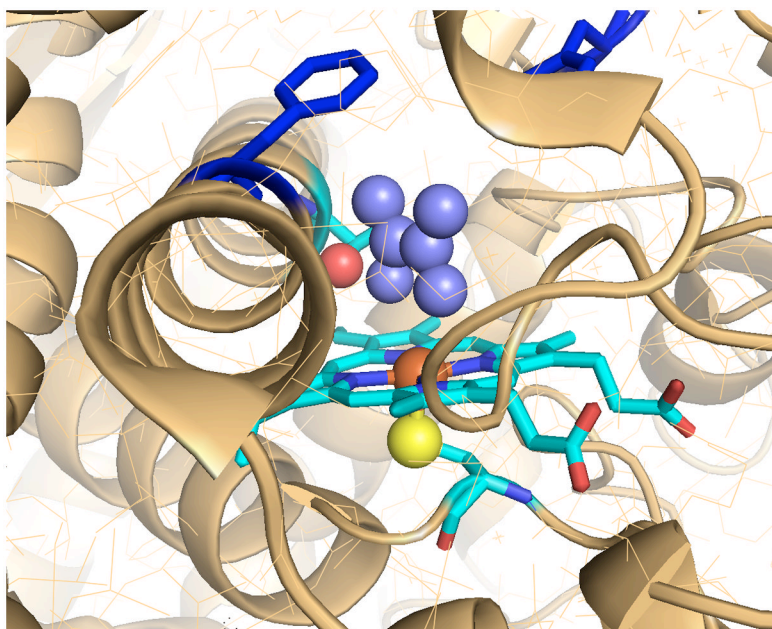


Figure 5. Active site of CYP2E1 with a modeled substrate, tetramethylethylene (medium blue). The figure illustrates constrictions between the active site, the small distal void, and the substrate access channel (top left). The phenyl substituent of F298 in the I helix (dark blue) forms a cap above the active site. Rotation of this group by about 90° , which has been observed for longer substrates, opens the active site to the substrate channel. The heme (light blue), iron (orange), axial thiolate ligand (yellow) and threonine hydroxyl (red) are also depicted. Created with MacPyMol from 3E61.pdb, cf. references ⁵⁵ and ⁵⁶.

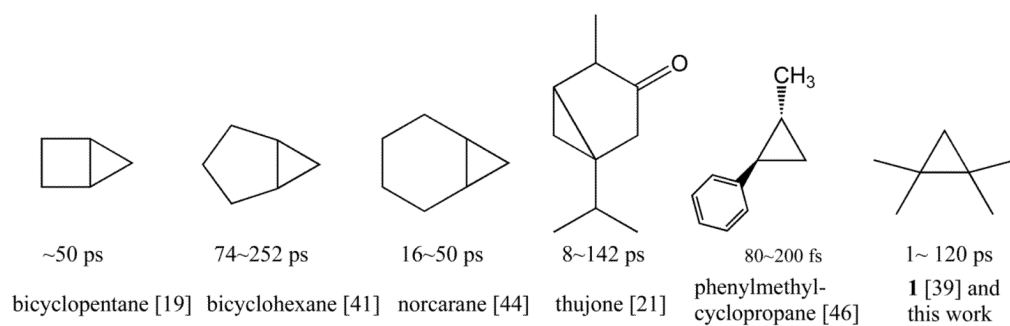
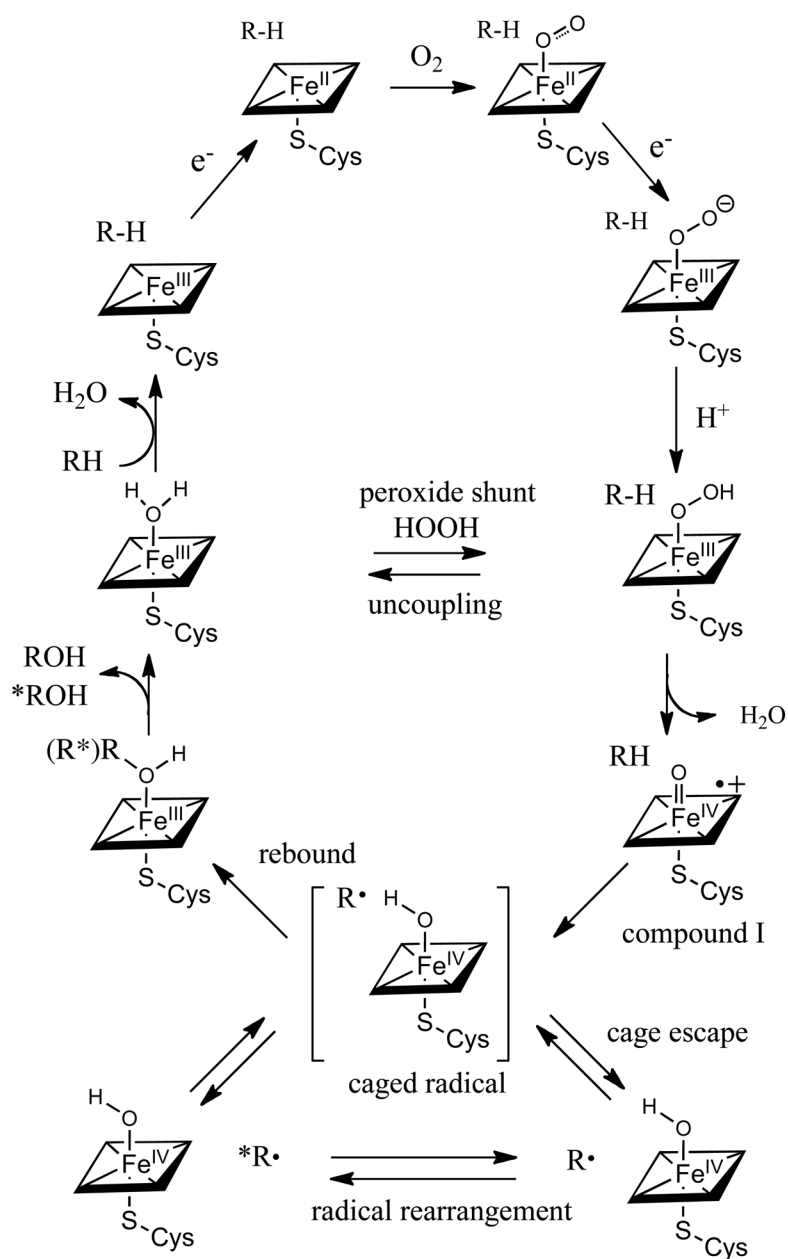
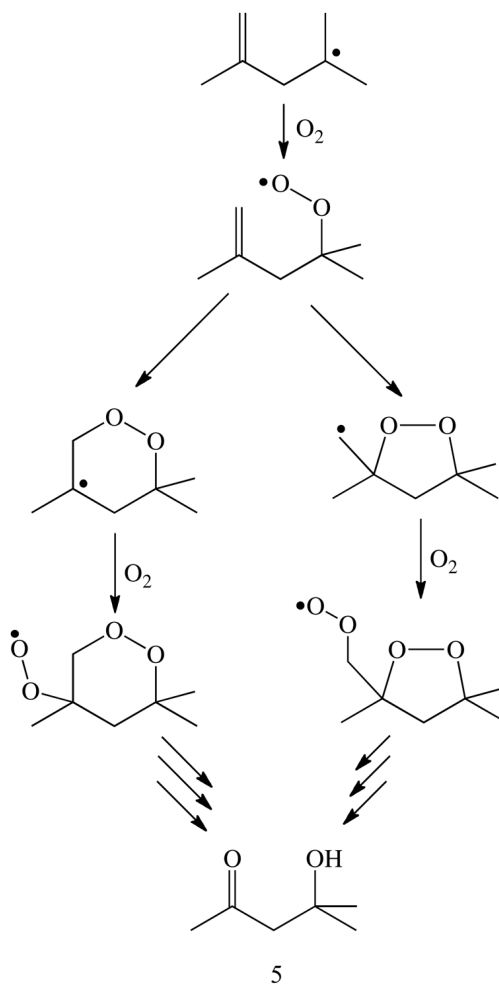


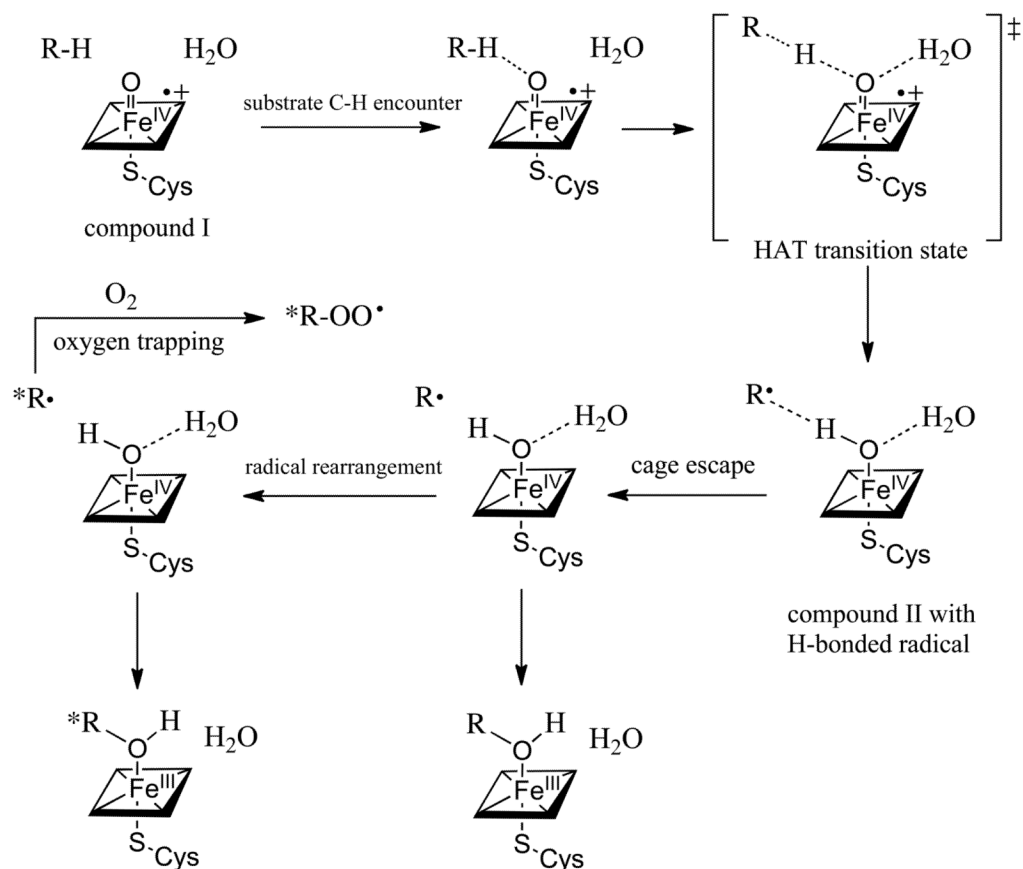
Figure 6. Apparent lifetimes of intermediate cyclopropylcarbinyl radicals as determined from rearranged products in reactions mediated by cytochrome P450 enzymes.

**Scheme 1.**

Cytochrome P450 catalytic cycle, with emphasis on the oxygen rebound step, showing the rearrangement of the radical intermediate, which could occur either within the initial cage or after cage escape.



Scheme 2.
Possible oxygen-trapping pathways to diacetone alcohol (5).

**Scheme 3.**

Depiction of a cage recombination-cage escape scenario for oxygen rebound by cytochrome P450. The intermediates, in sequence, are compound I (oxoiron(IV) porphyrin radical cation) with the substrate and peroxide-derived water at the active site; C-H encounter via π^* -approach to the ferryl; the hydrogen abstraction (HAT) transition state; compound II with a hydrogen bond to the incipient substrate radical R^\bullet ; cage escape of the radical and rearrangement or oxygen rebound to form either rearranged or unrearranged product alcohol coordinated to the heme iron(III).

Table 1

Results of P450 catalyzed oxidation of TMCP.

Enzyme	Human CYP2E1	Human CYP3A4	Rat CYP2B1
Product	Yield (%) ^a	Yield (%) ^a	Yield (%) ^b
2	80	96	99.7
3	nd ^c	1.6	0.1
4	nd ^c	1.1	0.2
5	20	1.6	trace
Conversion	4%	17%	86%
Activity ^d	90	800	2000
U/R ^e	4.5 ± 1.5	36 ± 2	750 ± 250
Rebound rate	0.9×10 ¹⁰ ± 0.3×10 ¹⁰ s ⁻¹	7.2×10 ¹⁰ ± 0.4×10 ¹⁰ s ⁻¹	1×10 ¹² ± 1×10 ¹¹ s ⁻¹
Radical lifetime	120 ± 40 ps	13 ± 1 ps	1 ± 0.3 ps

^a average of 3 runs;^b average of 2 runs;^c nd, not detected;^d nmol/min/nmol P450;^e ratio of unrearranged (**2+3**) to rearranged (**4+5**) products.